Iranian Polymer Journal (2021) 30:697–705
https://doi.org/10.1007/s13726-021-00924-x

ORIGINAL RESEARCH

Methacrylate-functionalized POSS influence on cross-linking and mechanical properties of styrene-butadiene rubber

Seda Bekin Acar[1,2] · Mehmet Atilla Tasdelen[1] · Bagdagul Karaagac[3]

Received: 23 October 2020 / Accepted: 14 April 2021 / Published online: 22 April 2021

Abstract

The addition of methacrylate-functional polyhedral oligomeric silsesquioxane (MA-POSS) nanoparticles to styrene-butadiene rubber (SBR) composites was evaluated in terms of rheological, mechanical, and morphological properties. The aging process and cross-link density of rubber nanocomposites were examined in presence of MA-POSS. The MA-POSS could directly participate in the vulcanization reaction due to its methacrylate groups and its concentration affected the rheological and mechanical properties of rubber. The sulfur vulcanization characteristics of MA-POSS/SBR nanocomposites were determined by moving die rheometer. It was indicated that the addition of MA-POSS to SBR composites retarded the curing time and decreased the cross-link density. Due to an effective interaction between MA-POSS nanofiller and SBR matrix and excellent dispersion of POSS, the mechanical properties of nanocomposites were higher than those of the reference compound without MA-POSS. However, there was no significant change investigated in tensile retention in presence of MA-POSS. The presence and the random distribution of MA-POSS in SBR matrix was confirmed by TEM analysis. The cross-link densities of the composites, which were calculated using Flory–Rehner equation, decreased with increasing amount of POSS nanofiller. It was finally revealed that the thermal aging dramatically reduced the mechanical properties and cross-link density of MA-POSS/SBR nanocomposites.

Keywords In situ polymerization · Nanocomposites · Polyhedral oligomeric silsesquioxane · Rubber · Styrene-butadiene copolymer

Introduction

Styrene-butadiene rubber (SBR) is a copolymer of styrene and butadiene and has been widely used as a synthetic non-polar rubber in various industries such as automobile and truck tires, cables and wires, and conveyor belts [1–3]. The tire industry is particularly dependent on SBR owing to its high wet grip, low rolling resistance, good incision impedance, abrasion and weather resistance, high filler loading capacity properties [4, 5]. However, the use of SBR has suffered from several drawbacks, including poor mechanical properties, low resilience and tear strength, and short lifetime due to its high level fatigue [6]. To overcome these disadvantages, it is generally reinforced with various additives such as carbon black, silica particles, metal oxides, etc. [4]. For instance, the incorporation of inorganic fillers such as MgO, $Mg(OH)_2$, or $BaSO_4$ in the presence of methacrylic acid have significantly improved the tensile strength, tear strength and modulus of the SBR [7–9].

Polyhedral oligomeric silsesquioxanes (POSSs) [10–12] are three-dimensional nanofillers composed of inner inorganic silicon and oxygen cage-like core and external organic groups. POSSs are one of the most popular new generation of nanofillers with their ability to stabilization and reinforcement of polymer matrices [13–15]. Due to their hybrid structures and diverse functionalities, the POSS molecules are well combined with polymer/rubber composites [16–18] by either physical blending with polymer matrix [19] or chemical bonding with polymer chain to form rigid cross-linking in the polymer network [20, 21]. In the literature, limited number of studies have been reported on

✉ Mehmet Atilla Tasdelen
tasdelen@yalova.edu.tr

[1] Department of Polymer Materials Engineering, Faculty of Engineering, Yalova University, 77200 Yalova, Turkey

[2] Institue of Science, Yalova University, 77200 Yalova, Turkey

[3] Department of Chemical Engineering, Engineering Faculty, Kocaeli University, 41380 Kocaeli, Turkey

the preparation of SBR/POSS nanocomposites [22, 23]. For instance, D'Arienzo et al. grafted different amounts of octamethacryl POSS (MA-POSS) onto silanized commercial SiO_2, using a surface reaction mediated by dicumyl peroxide as a radical initiator and utilized them as reinforcement for SBR matrix by ex situ blending method. It was found that modulus increased and hysteresis decreased in the presence of hybrid SiO_2/POSS nanofiller that provided a positive effect on mechanical properties for SBR matrix [22]. The methacryl functionalities of SiO_2/POSS promoted the cross-linking reactions in proximity of the filler surfaces, and gave rise to form a strict network bonded to the rubber chains [23]. All these results suggest that the contribution of MA-POSS nanofiller alone should be investigated as the cage interaction with the rubber matrix.

In this study, we report on the promising properties of MA-POSS, having multifunctional methacrylate groups as nanosized reinforcement particles and an effective co-cross-linker for SBR compounds. The amount of MA-POSS varied between 1 and 5 phr as the experimental parameter. Sulfur was used as cross-linking agent and its content was 1.5 phr in all composite recipes. It was aimed that MA-POSS could contribute to the cross-linking of SBR with sulfur because of having –C=C– bonds in its structure. The obtained SBR/MA-POSS nanocomposites were compared with the reference compound prepared without nanofiller in terms of rheological, mechanical, and morphological properties. The effects of MA-POSS on thermal aging and cross-link density of SBR were also investigated.

Experimental

Materials

Styrene-butadiene rubber (SBR 1502) with a styrene content of 27% was obtained from Arlanxeo, Germany. Octa(propylmethacryl) POSS (MA-POSS), a viscous liquid at ambient conditions, with a molecular weight of 1433.97 g/mol was purchased from Hybrid Plastics Inc., USA and used without further purification. Zinc oxide (ZnO), stearic acid (SA), 2,2,4-trimethyl-1,2-dihydroquinoline (TMQ), n-isopropyl-n'-phenyl 1,4-phenylenediamine (IPPD), ozone wax, tetramethylthiuram disulfide (TMTD), *N*-cyclohexyl-2-benzothiazole sulfenamide (CBS), and sulfur (S) were purchased from Rubber Chem, Turkey and used as received.

Experimental procedure

The recipe of rubber compounds is given in Table 1. MA-POSS content was selected as 1, 3, and 5 phr. The composite mixes were prepared using Brabender® laboratory type banbury mixer at 50 rpm rotor speed. First, SBR was masticated in the banbury mixer for 2 min. Then, MA-POSS nanofiller was added to SBR and mixed for 1 min. The ZnO and stearic acid were added and mixed for 0.5 min. TMQ, IPPD and ozone wax were added as stabilizers and mixed for 0.5 min further. Finally, TMTD, CBS and S were added and mixed for 1 min. The compound was dropped from the mixer after 5 min total mixing cycle at approximately 80 °C. Vulcanization process was carried out using a hydraulic hot press at 160 °C. The cure parameters were investigated and analyzed by a moving die rheometer (MDR). Test specimens were cut from the molded sheets into required dimensions by standard blades. The thermal aging of rubber composites was carried out in an air-circulating oven at 70 °C for 70 h to investigate its effect on structural and mechanical properties, and cross-link density of composites.

Table 1 Rubber compound formulations

Component	Content (phr)	Component	Content (phr)
SBR	100	IPPD	1
MA-POSS	0/1/3/5	Ozone wax	1
ZnO	5	TMTD	1
SA	2	CBS	1
TMQ	1	S	1.5

Characterization

Important rheological parameters and optimum curing times of the compounds were determined by a moving die rheometer (MDR, Alpha Technologies) analysis according to ASTM D5289, 2019.

Fourier-transform infrared spectra of rubber composites were obtained by a Perkin-Elmer Spectrum Two Spectrometer (Lambda 25, Waltham, MA, USA) equipped with a diamond attenuated total reflectance (ATR) device at ambient temperature.

Tensile properties of reference compound and SBR/MA-POSS nanocomposites were examined using an Instron Universal Testing Machine (Model 3345) according to ASTM D412. The crosshead speed was set to 500 mm/min. Hardness of cured composites were measured by Zwick Shore A type durometer according to ASTM D2240, 2015. Compression set test was conducted appropriately with ASTM D395, 2018.

The transmission electron microscopy (TEM) analysis was carried out using a Jeol JEM-2100 (UHR) Gatan, (USA) at 300 kV to visualize average nanofiller distribution and morphology of the rubber nanocomposites.

The cross-link densities of the vulcanized and aged samples were calculated on the principle of equilibrium solvent-swelling measurements by applying a well-known modified Flory–Rehner equation for tetra-functional networks.

Samples having 2-mm thicknesses were initially weighed (m_i) and immersed in toluene for 72 h at room temperature. The swollen samples were taken out and carefully dried to remove excess solvent before being weighed (m_g). Solvent residues and other small molecules were eliminated by drying in an air-circulating oven at 70 °C for 24 h. At the end, the samples were weighed for the last time (m_s). Volume fractions of polymer in the samples at equilibrium swelling (ν_{2m}) were determined from swelling ratio G, and calculated with the following equations:

$$\nu_{2m} = \frac{1}{1+G}, \tag{1}$$

where

$$G = \frac{m_g - m_s}{m_s} \times \frac{\rho_r}{\rho_s}, \tag{2}$$

where ρ_r and ρ_s represent the densities of rubber samples and solvent, respectively.

The cross-link densities of the samples (ν) were determined from swelling measurements in toluene as solvent using Flory–Rehner relation and calculated with the following equation [24]:

$$\nu = -\frac{\ln\left(1-\nu_{2m}\right) + \nu_{2m} + \chi\nu_{2m}^2}{V_1\left(\nu_{2m}^{\frac{1}{3}} - \frac{2}{\phi}\nu_{2m}\right)}, \tag{3}$$

where V_1 is the molar volume of solvent (106.35 cm^3/mol for toluene [25]), χ is the polymer–solvent interaction parameter (0.378 for SBR-toluene) [8, 25, 26], and $\phi = 4$ is the cross-link functionality [24].

Results and discussion

Reaction mechanism

Vulcanization mechanism of rubber is complicated and includes a combination of radical and polar interactions. The cross-linking can be achieved by reactions of several atoms including a carbon-to-carbon bond with a group of sulfur atoms in a short chain, a single sulfur atom, a polyvalent organic radical, a polyvalent metal ion or an ionic cluster. In our case, a proposed reaction mechanism between sulfur and MA-POSS is given in Scheme1. The vulcanization occurs in two steps: (1) generation of active-sulfurating agents and (2) cross-linking reaction taking place between an activated sulfurating species and unsaturated double-bonds of either SBR or MA-POSS. First, an active accelerator complex was formed with the reaction of CBS (accelerator) with ZnO (activator). This complex reacted with S_8 to form sulfurating species. The following multi-step reactions between the activated sulfurating species with unsaturated sites of MA-POSS led to the inclusion of MA-POSS into the SBR system as shown in Scheme 1 [27]. As a result, the octa-methacrylate-functional MA-POSS was accompanied with vulcanization reaction between rubber chains and acted as both nanofiller and cross-linker in the obtained SBR nanocomposites.

Cure characteristics

The rheometer data for the reference sample and SBR/MA-POSS nanocomposites obtained at 160 °C and important parameters including minimum and maximum torque values (ML and MH), scorch time (t_{s2}), optimum cure time (t_{90}), cure rate index (CRI), and cure extent (CE) are summarized in Table 2. Three rheometer tests were performed for each compound and the average results were given. The ML values of all nanocomposites, which were proportional to compound viscosity, were almost similar with the reference sample's value, whereas the MH values decreased by increasing MA-POSS concentration up to 3 phr. Upon

Scheme 1 Possible reaction mechanism of MA-POSS and sulfur

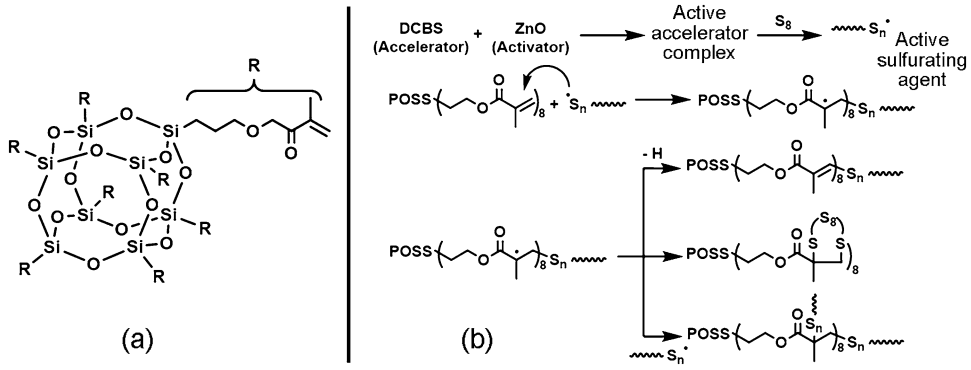

Table 2 Rheological properties of reference compound and SBR/MA-POSS nanocomposites

Samples	ML (dNm)	MH (dNm)	CE (dNm)	t_{s2} (min)	t_{90} (min)	CRI (min^{-1})
Reference	0.64	11.11	10.47	1.98	3.68	58.82
SBR/MA-POSS-1	0.63	10.68	10.05	1.81	3.58	56.66
SBR/MA-POSS-3	0.63	8.05	7.42	2.63	5.22	38.54
SBR/MA-POSS-5	0.61	8.78	8.17	2.17	5.18	40.14

higher addition of MA-POSS, this value slightly increased in the case of 5 phr, but it was still lower than that of the reference sample. In the literature, the CE value is closely related to cross-linking degree of the rubber and obtained from the difference between MH and ML values [11]. The CE value of reference sample was found as 10.47 dNm and it was decreased simultaneously with increasing amount of MA-POSS up to 3 phr. This could be due to the bulky POSS cages which not only increase steric hindrance between the double-bonds and sulfur atoms but also decrease their cross-link density in the final SBR/MA-POSS nanocomposites. In the case of higher MA-POSS, the CE values were slightly higher than the SBR/MA-POSS-5 sample that was attributed to the agglomerate formation of POSS nanoparticles. Also, the optimum curing time (t_{90}) increased by increasing amount of MA-POSS. The differences in terms of relative cross-link density and optimum curing time in the presence of MA-POSS could be associated with the dominating reaction between MA-POSS and sulfur, in which sulfur was consumed at the early stage of the vulcanization. Therefore, the incorporation of MA-POSS caused a retarding effect on cross-linking of rubber composites. On the other hand, the cure rate index (CRI) values were calculated according to the following equation:

$$\mathrm{CRI} = \frac{100}{t_{90} - t_{s2}}. \tag{4}$$

As shown in Table 2, CRI values exhibited a decrease with MA-POSS addition up to 3 phr. A longer curing time and higher CRI values implied that the vulcanization reaction mechanism of SBR was completely changed in the presence of MA-POSS compounds. The decrease in CRI values during vulcanization reaction generally implies that there is lower cross-linking density [11] in the SBR/MA-POSS nanocomposites.

FTIR characterization

The incorporation of the MA-POSS in the SBR matrix was checked by FTIR spectroscopy equipped with an ATR tool measuring. FTIR spectra of the reference and SBR/MA-POSS-1 samples are given in Figs. 1 and 2. The peaks existing in the 3400–3450 cm^{-1} in FTIR spectrum of reference sample were assigned to the stretching vibrations of O–H

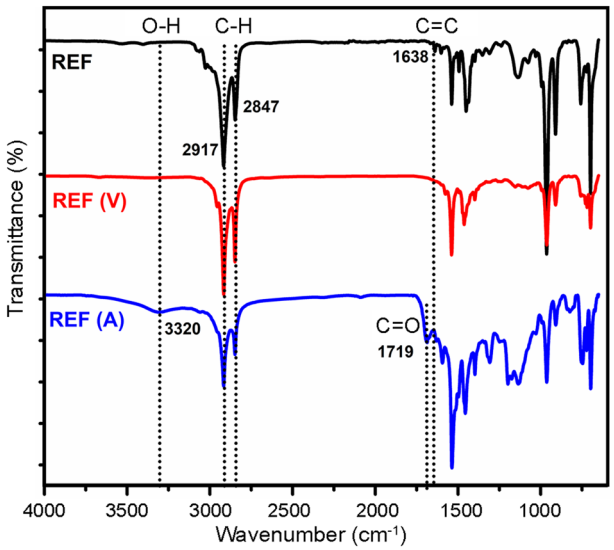

Fig. 1 FTIR spectra of the reference compound with non-vulcanizate, vulcanizate (V) and aged (A) steps

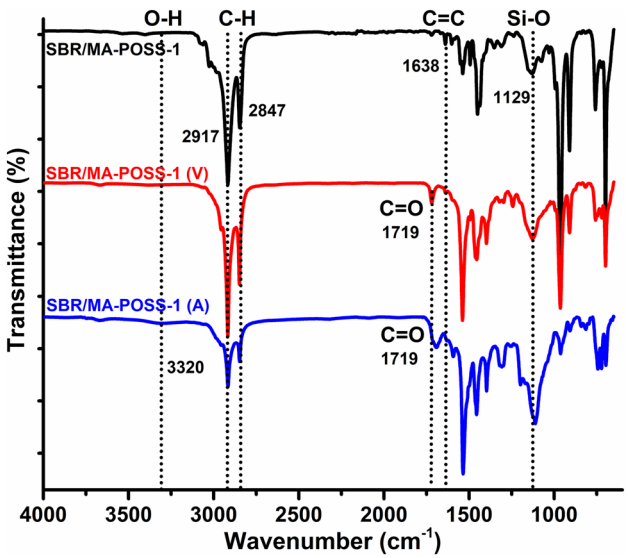

Fig. 2 FTIR spectra of SBR/MA-POSS-1 nanocomposite with non-vulcanizate, vulcanizate (V) and aged (A) steps

bonds. The small peak at 3023 cm^{-1} corresponded to the aromatic C–H stretching. The bands at 2917 and 2847 cm^{-1} were attributed to the aliphatic C–H stretching due to the

vinyl group present in the SBR chain. Also, the absorption band at 1638 cm^{-1} was assigned to the stretching vibration of C=C band. The bands at 1451 and 1396 cm^{-1} were due to the asymmetric and symmetric bending vibrations of C–H bond, while the band at 1075 cm^{-1} was due to the stretching vibration of C–O bond. In addition, the peaks at 964, 758, and 694 cm^{-1} were attributed to trans 1,4 –C=C out-of-plane deformation of butadiene, C=C groups of polystyrene belonging to SBR, and the out-of-plane vibrations of aromatic =C–H, respectively [4, 8, 28]. In the FTIR spectrum of vulcanizate reference sample, there was no peak at 1638 cm^{-1}, which confirmed the successful vulcanization process (REF V). Also, the increasing intensity of the peaks of hydroxyl and carbonyl bonds confirmed the oxidative aging in the FTIR spectrum of aged reference sample (REF A) (Fig. 1).

In the FTIR spectrum of SBR/MA-POSS-1 nanocomposite (Fig. 2), a new peak appeared at 1129 cm^{-1}, which was attributed to the stretching vibration of Si–O bond of POSS groups, and it confirmed the presence of MA-POSS in the rubber nanocomposite [29–31]. Moreover, the band at 1719 cm^{-1} was attributed to C=O bond due to the methacrylate group of MA-POSS in the SBR/MA-POSS-1. In the spectra of vulcanizate and aged nanocomposites, there was no peak at 1638 cm^{-1} belonging to C=C stretching in the spectrum of aged SBR/MA-POSS-1 (A). Also, the intensity of the peaks of hydroxyl and carbonyl bonds increased after the oxidative aging of the nanocomposite (Fig. 2). After the thermal oxidation process, which occurred in the backbone chains and vinyl pendants of SBR, the oxygen containing molecules such as alcohols, ethers or esters were readily formed [32].

Mechanical properties

The mechanical properties of vulcanizate and aged SBR nanocomposites are given in Fig. 3 and Table 3. Mechanical tests were performed five times for each sample and the averaged results were presented with standard deviation. It was revealed that the tensile strengths of SBR/MA-POSS nanocomposites were slightly higher than those of the reference compound. With further MA-POSS addition, the tensile properties of the nanocomposites were increased from 1.41 to 1.56 MPa, which accounted for 10.6% improvement. The distribution of POSS nanoparticles in the cross-linked three-dimensional networks, interaction between polymer matrix and filler/nanofiller, and particle dispersion/agglomeration have crucial importance for the mechanical properties of

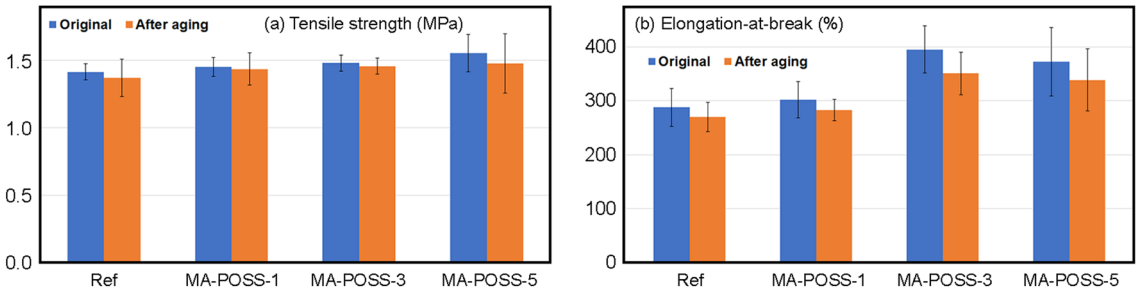

Fig. 3 Tensile strength **a** and elongation-at-break, **b** of the vulcanizated and aged samples

Table 3 FTIR peaks of the reference compound and SBR/MA-POSS-1 nanocomposite

Band origin	Wavenumbers of samples (cm^{-1})	
	Reference	SBR/MA-POSS-1
O–H stretching	3400–3450	3400–3450
C–H stretching	2917 and 2847	2917 and 2847
C=O stretching	1719	1719
C=C stretching	1638	No peak
Asymmetric bending vibrations of C–H	1451	1452
Symmetric bending vibrations of C–H	1396	1396
Si–O stretching of POSS groups	no peak	1129
C–O stretching	1075	1075
Trans 1,4 –C=C out-of-phase deformation of butadiene	964	964
C=C groups of polystyrene belonging to SBR	758	758
Out-of-plane vibrations of aromatic =C–H	694	694

rubber composites. In this case, an effective interaction between MA-POSS nanofiller and SBR matrix provided enhanced mechanical strength. Moreover, elongation-at-break values increased with increasing amount of POSS up to 3 phr. It decreased slightly about 5.8% with 5 phr MA-POSS addition, which could be attributed to possible MA-POSS agglomerations or lower cross-linking degree of the SBR/MA-POSS-5 nanocomposite. This result was also confirmed by previous rheometer results (Table 2). However, it was still higher than that of reference sample.

The 50% tensile modulus and Shore A hardness values of SBR/MA-POSS nanocomposites were slightly lower than those of the reference sample (Fig. 4). Based on previous results, the incorporation of MA-POSS not only led to a drop in cross-link density but also lower modulus and hardness of the nanocomposites therewith. On the other hand, after thermal aging in air, the tensile strength and elongation-at-break values decreased, but the modulus and Shore A hardness of reference compound and rubber nanocomposites increased due to increased rigidity, as expected [33–35]. This result was in good agreement with the findings of Schaefer et al. who reported that the rigidity of three-dimensional polymer networks led to an increase in the modulus of composites [36].

Compression set test was carried out at room temperature for 22 hand at 70 °C for 70 h according to method B (ASTM D395, 2018) [37] to determine the effect of MA-POSS loading on the permanent deformation of compounds and to retain their elastic properties after prolonged compression. It was found that the compression set values of nanocomposites were significantly increased as MA-POSS loading increased in vulcanizate and aged samples compared to the reference sample (Table 4). Furthermore, the loss of elastic properties and an increase of compression set proved the reduction in the cross-link density of the nanocomposites.

Morphology

A good dispersion of nanofillers as well as strong interfacial interactions between POSS nanoparticles and polymer/rubber matrix have a crucial effect on thermal, mechanical, physical and flammability properties of nanocomposites [30, 31, 38, 39]. The morphology of the nanocomposites and the distribution level of MA-POSS in SBR matrix were

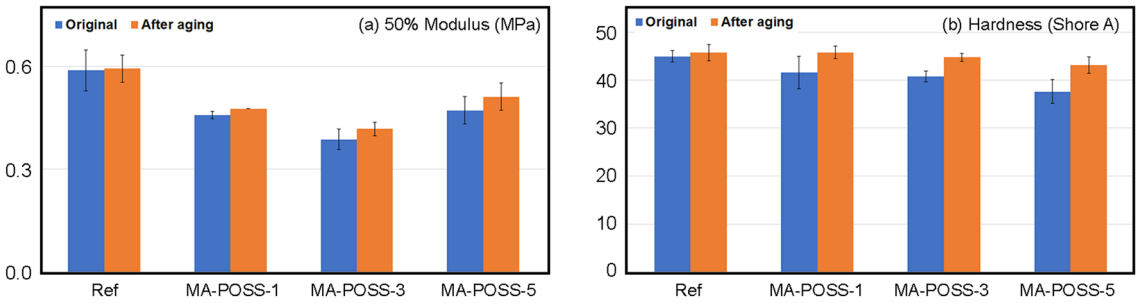

Fig. 4 Tensile modulus at 50% and hardness of the vulcanizate and aged samples

Table 4 The mechanical properties of vulcanizate and aged samples

Samples	Tensile strength[b] (MPa)	Elongation-at-break[b] (%)	Modulus[b] (MPa)	Hardness[c] (shore A)	Compression set[d] (%)
Reference	1.41 ± 0.06	288 ± 35	0.59 ± 0.06	45.0 ± 1.2	5.7 ± 0.8
Reference (A)[a]	1.37 ± 0.14	270 ± 27	0.59 ± 0.04	45.8 ± 1.7	20.5 ± 2.1
SBR/MA-POSS-1	1.45 ± 0.07	302 ± 34	0.46 ± 0.01	41.6 ± 3.4	6.6 ± 1.2
SBR/MA-POSS-1 (A)[a]	1.44 ± 0.12	283 ± 20	0.48 ± 0.00	45.8 ± 1.3	27.7 ± 3.5
SBR/MA-POSS-3	1.48 ± 0.06	396 ± 43	0.39 ± 0.03	40.8 ± 1.1	6.9 ± 1.0
SBR/MA-POSS-3 (A)[a]	1.46 ± 0.06	351 ± 39	0.42 ± 0.02	45.8 ± 0.8	30.8 ± 2.8
SBR/MA-POSS-5	1.56 ± 0.14	373 ± 64	0.47 ± 0.04	37.6 ± 2.5	7.1 ± 1.7
SBR/MA-POSS-5 (A)[a]	1.48 ± 0.22	339 ± 57	0.51 ± 0.04	43.2 ± 1.7	35.2 ± 4.9

[a](A): aged samples

[b]According to ASTM D412, 2016

[c]According to ASTM D2240, 2015

[d]According to ASTM D395, 2018

evaluated by TEM analysis. According to tensile test, SBR/MA-POSS-5 showed the best mechanical performance. Therefore, MA-POSS might be well dispersed in the SBR nanocomposite and this should be investigated in terms of morphological properties. TEM micrographs of SBR/MA-POSS-5 sample exhibited rather continuous and homogeneous distribution and some very rare aggregates of POSS that could be seen as black cluster between 50 and 200 nm (shown in Fig. 5a). This case of MA-POSS in SBR matrix could be associated with the difference of surface energies [40]. Furthermore, with higher magnification (Fig. 5b), spherical POSS nanoparticles with a diameter ranging from 2 to 5 nm were randomly dispersed, which was close to the dimensions of a single POSS molecule. However, there were still some agglomerated POSS nanoparticles present in the SBR/MA-POSS-5 sample. Consequently, the TEM results confirmed the presence of POSS nanoparticles as well as their random distributions in the SBR matrix.

Cross-link density

The cross-link densities (ν) of both vulcanizates and aged samples calculated using Flory–Rehner equation are given in Fig. 6. The presented results were average values of three experiments. It was indicated that the cross-link density of composites decreased with increasing amount of POSS nanofiller. This result confirmed the rheological and mechanical data. On the other hand, the aging of nanocomposite samples also significantly reduced cross-link density of samples by increasing POSS nanofiller content. This could be attributed to possible chain breaks caused by heat during thermal aging.

Conclusion

This is an account on the influence of MA-POSS as a nano-sized reinforcement for SBR matrix. The sulfur curing characteristics of composites were determined by means of rheology and solvent-swelling measurements. It was found that MA-POSS retarded the curing time and decreased cure extent value closely related to cross-linking degree of the rubber. These results could be associated with the dominating reaction between MA-POSS and sulfur, in which sulfur was consumed at early stage of vulcanization reaction. Mechanical tests showed that tensile strength was improved with MA-POSS loading, which could be attributed to good interaction between MA-POSS nanoparticles and SBR matrix. Cross-link density of the nanocomposites calculated with Flory–Rehner equation decreased with increasing loading of MA-POSS nanofiller. TEM images of rubber nanocomposite at 5 phr MA-POSS confirmed the presence and random distribution of MA-POSS in the SBR matrix. After thermal aging in air, mechanical properties of rubber composites were deteriorated and material rigidity increased as expected, which could be assigned to possible chain breaks caused by heat. However, there was no significant

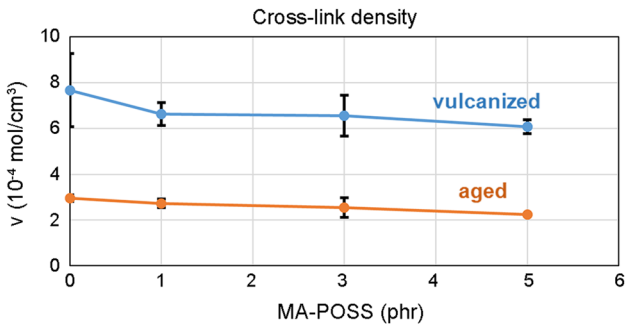

Fig. 6 Cross-link densities of vulcanizate and aged samples

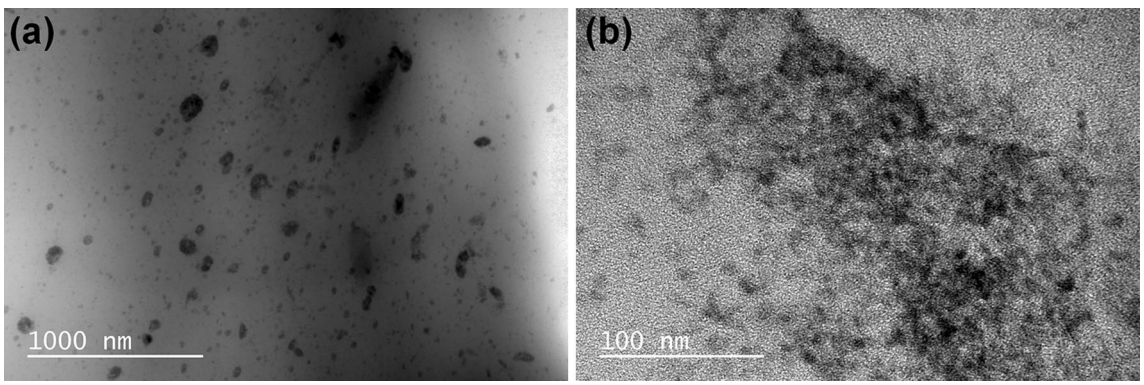

Fig. 5 TEM images of SBR/MA-POSS-5 at low **a** and high **b** magnifications

change investigated in tensile retention in the presence of MA-POSS.

Acknowledgements This work was supported by the Scientific Research Fund of Yalova University (Project No.: 2018/DR/0007) for the financial support.

References

1. Alwaan IM (2020) Evaluation of morphological, mechanical, and rheological properties of vulcanized styrene–butadiene rubber/modified corn starch blends. Polym Polym Compos 28:45–53
2. Raslan HA, El-Saied HA, Yousif N (2019) Gamma radiation induced fabrication of styrene butadiene rubber/magnetite nanocomposites for positive temperature coefficient thermistors application. Compos B 176:107326
3. Xu Z, Jerrams S, Guo H, Zhou Y, Jiang L, Gao Y, Zhang L, Liu L, Wen S (2020) Influence of graphene oxide and carbon nanotubes on the fatigue properties of silica/styrene-butadiene rubber composites under uniaxial and multiaxial cyclic loading. Int J Fatigue 131:105388
4. Khalifeh S, Tavakoli M (2019) Styrene butadiene rubber/epoxidized natural rubber/carbon filler nanocomposites: microstructural development and cure characterization. Iran Polym J 28:1023–1033
5. Nawwar G, Yakout S, El-Sadiek M, El-Sabbagh S (2011) Synthesis and evaluation of new antioxidants for styrene butadiene rubber. Pigm Resin Technol 40:399–409
6. Sahakaro K (2017) Mechanism of reinforcement using nanofillers in rubber nanocomposites. Progress in rubber nanocomposites. Elsevier, pp 81–113
7. Yin D, Zhang Y, Peng Z, Zhang Y (2003) Effect of fillers and additives on the properties of SBR vulcanizates. J Appl Polym Sci 88:775–782
8. Khan M, Mishra S, Ratna D, Sonawane S, Shimpi NG (2019) Investigation of thermal and mechanical properties of styrene–butadiene rubber nanocomposites filled with SiO_2–polystyrene core–shell nanoparticles. J Compos Mater 54:1785–1795
9. Alimardani M, Abbassi-Sourki F, Bakhshandeh GR (2012) Preparation and characterization of carboxylated styrene butadiene rubber (XSBR)/multiwall carbon nanotubes (MWCNTs) nanocomposites. Iran Polym J 21:809–820
10. Liu K, Lu S, Li S, Huang B, Wei C (2012) Mechanical and thermal properties of POSS-*g*-GO reinforced epoxy composites. Iran Polym J 21:497–503
11. Sirin H, Kodal M, Karaagac B, Ozkoc G (2016) Effects of octamaleamic acid-POSS used as the adhesion enhancer on the properties of silicone rubber/silica nanocomposites. Compos B 98:370–381
12. Hou G, Li N, Han H, Huo L, Gao J (2015) Hybrid cationic ring-opening polymerization of epoxy resin/glycidyloxypropyl-polyhedral oligomeric silsesquioxane nanocomposites and dynamic mechanical properties. Iran Polym J 24:299–307
13. Liu Q, Ren W, Zhang Y, Zhang Y (2012) A study on the curing kinetics of epoxycyclohexyl polyhedral oligomeric silsesquioxanes and hydrogenated carboxylated nitrile rubber by dynamic differential scanning calorimetry. J Appl Polym Sci 123:3128–3136
14. Ozdogan R, Daglar O, Durmaz H, Tasdelen MA (2019) Aliphatic polyester/polyhedral oligomeric silsesquioxanes hybrid networks via copper-free 1,3-dipolar cycloaddition click reaction. J Polym Sci Part A Polym Chem 57:2222–2227
15. Doganci E, Uner A, Canimkurbey B, Ozdogan R, Tasdelen MA (2018) Star-shaped hybrid polymers as insulators for organic field effect transistors. Polym Adv Technol 29:3020–3026
16. Yazıcı N, Dursun S, Yarıcı T, Kılıç B, Mert O, Bdl K, Gr Ö, Kodal M (2020) Effect of octavinyl-polyhedral oligomeric silsesquioxane on the cross-linking, cure kinetics, and adhesion properties of natural rubber/textile cord composites. Ind Eng Chem Res 59:1888–1901
17. Sahoo S, Bhowmick AK (2007) Polyhedral oligomeric silsesquioxane (POSS) nanoparticles as new crosslinking agent for functionalized rubber. Rubber Chem Technol 80:826–837
18. Lakshmipriya S, Anil Kumar S, Nandakumar K, Thomas S (2019) Influence of POSS fillers on the transport properties of natural rubber nanocomposites. Polym Compos 40:3020–3031
19. Ayandele E, Sarkar B, Alexandridis P (2012) Polyhedral oligomeric silsesquioxane (POSS)-containing polymer nanocomposites. Nanomaterials 2:445–475
20. Arslan I, Tasdelen MA (2016) POSS-based hybrid thermosets via photoinduced copper-catalyzed azide–alkyne cycloaddition click chemistry. Des Monomers Polym 19:155–160
21. Sencevik RG, Tasdelen MA (2014) Poly(methyl methacrylate)/POSS hybrid networks by type II photoinitiated free radical polymerization. Polym Compos 35:1614–1620
22. D'Arienzo M, Redaelli M, Callone E, Conzatti L, Di Credico B, Dire S, Giannini L, Polizzi S, Schizzi I, Scotti R (2017) Hybrid SiO_2@ POSS nanofiller: a promising reinforcing system for rubber nanocomposites. Mater Chem Front 1:1441–1452
23. Redaelli M, D'Arienzo M, Brus J, Di Credico B, Geppi M, Giannini L, Matejka L, Martini F, Panattoni F, Spirkova M (2018) On the key role of SiO_2@ POSS hybrid filler in tailoring networking and interfaces in rubber nanocomposites. Polym Test 65:429–439
24. Stelescu MD, Manaila E, Craciun G (2013) Vulcanization of ethylene-propylene–terpolymer-based rubber mixtures by radiation processing. J Appl Polym Sci 128:2325–2336
25. Abd-El-Messieh S, Abd-El-Nour K (2003) Effect of curing time and sulfur content on the dielectric relaxation of styrene butadiene rubber. J Appl Polym Sci 88:1613–1621
26. Harandi MH, Alimoradi F, Rowshan G, Faghihi M, Keivani M, Abadyan M (2017) Morphological and mechanical properties of styrene butadiene rubber/nano copper nanocomposites. Results Phys 7:338–344
27. Ghosh P, Katare S, Patkar P, Caruthers JM, Venkatasubramanian V, Walker KA (2003) Sulfur vulcanization of natural rubber for benzothiazole accelerated formulations: from reaction mechanisms to a rational kinetic model. Rubber Chem Technol 76:592–693
28. Raef M, Razzaghi-Kashani M (2019) The role of interface in gas barrier properties of styrene butadiene rubber-reduced graphene oxide composites. Polymer 182:121816
29. Acar SB, Ozcelik M, Uyar T, Tasdelen MA (2017) Polyhedral oligomeric silsesquioxane-based hybrid networks obtained via thiol-epoxy click chemistry. Iran Polym J 26:405–411
30. Rybiński P, Syrek B, Bradło D, Żukowski W (2018) Effect of POSS particles and synergism action of POSS and poly-(melamine phosphate) on the thermal properties and flame retardance of silicone rubber composites. Materials 11:1298
31. Zhao L, Li J, Li Z, Zhang Y, Liao S, Yu R, Hui D (2018) Morphology and thermomechanical properties of natural rubber vulcanizates containing octavinyl polyhedral oligomeric silsesquioxane. Compos B 139:40–46
32. He S, Bai F, Liu S, Ma H, Hu J, Chen L, Lin J, Wei G, Du X (2017) Aging properties of styrene-butadiene rubber nanocomposites filled with carbon black and rectorite. Polym Test 64:92–100
33. Choi SS (2001) Influence of internal strain on change of crosslink density of natural rubber vulcanizates by thermal ageing. Polym Int 50:107–112
34. Choi SS (2000) Influence of rubber composition on change of crosslink density of rubber vulcanizates with EV cure system by thermal aging. J Appl Polym Sci 75:1378–1384

35. Barghamadi M, Karrabi M, Ghoreishy MHR, Mohammadian-Gezaz S (2019) Effects of two types of nanoparticles on the cure, rheological, and mechanical properties of rubber nanocomposites based on the NBR/PVC blends. J Appl Polym Sci 136:47550
36. Pan G, Mark JE, Schaefer DW (2003) Synthesis and characterization of fillers of controlled structure based on polyhedral oligomeric silsesquioxane cages and their use in reinforcing siloxane elastomers. J Polym Sci Part B Polym Phys 41:3314–3323
37. Mostafa A, Abouel-Kasem A, Bayoumi M, El-Sebaie M (2009) Effect of carbon black loading on the swelling and compression set behavior of SBR and NBR rubber compounds. Mater Des 30:1561–1568
38. Lipińska M, Imiela M (2019) Morphology, rheology and curing of (ethylene-propylene elastomer/hydrogenate acrylonitrile-butadiene rubber) blends reinforced by POSS and organoclay. Polym Test 75:26–37
39. Yang S, Fan H, Jiao Y, Cai Z, Zhang P, Li Y (2017) Improvement in mechanical properties of NBR/$LiClO_4$/POSS nanocomposites by constructing a novel network structure. Compos Sci Technol 138:161–168
40. Joshi V, Srividhya M, Dubey M, Ghosh A, Saxena A (2013) Effect of functionalization on dispersion of POSS-silicone rubber nanocomposites. J Appl Polym Sci 130:92–99